Imaging and time reversal in random media

George Papanicolaou
Department of Mathematics
Stanford University
http://georgep.stanford.edu

In collaboration with:

Liliana Borcea (CAM Rice), Chrysoula Tsogka (LMA-CNRS Marseille), James Berryman (LLNL), P. Blomgren (Math. Stanford), L. Ryzhik (Chicago), K. Solna (UCI), H. Zhao (UCI).

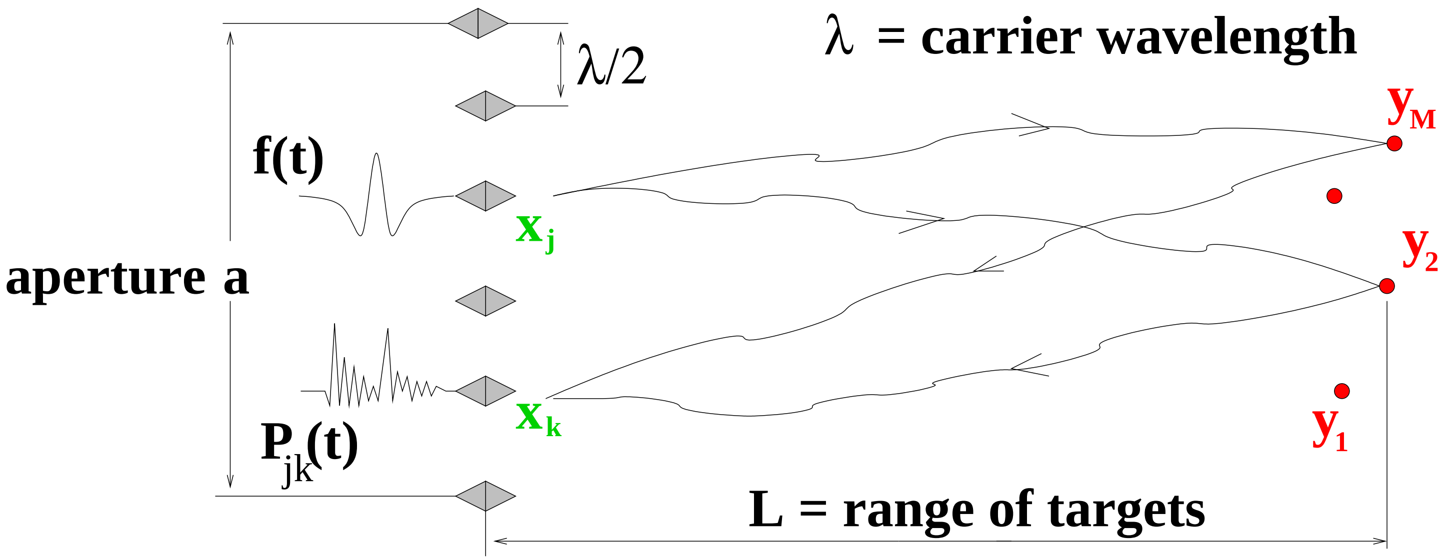

An array of N transducers probes a medium with M small scatterers with a pulse $f(t)$ emitted from transducer j, located at $\mathbf{x}_j$, and the echos $P_{jk}(t)$ are recorded at $\mathbf{x}_k$, for $k = 1, \ldots N$.

Imaging From the response matrix $\Big(P_{jk}(t)\Big)_{j,k=1\ldots N}$ find the number $M \leq N$ of scatterers and their location $\mathbf{y}_1, \mathbf{y}_2 \ldots \mathbf{y}_M$.

Random media In the regime $\lambda \leq l \ll a = N\lambda/2 \ll L$, where there is significant **multipathing**.

Imaging strategy

• **Imaging**: Requires some back propagation or **time reversal** of the measured fields into a medium (real or fictitious).

• Need to understand time reversal in random media.

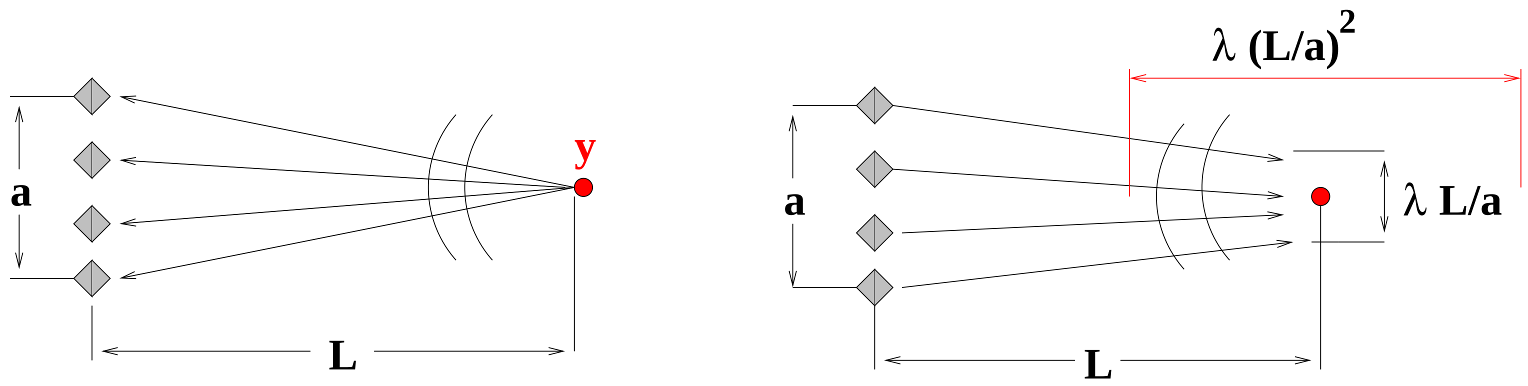

Significant **multipathing** in the random medium gives **super-resolution** and **statistical stabillity** of time reversal.

• **Our imaging approach**:
- To exploits super-resolution & statistical stability of time reversal.
- It is **coherent** (uses the phase of the measured field).

Applications of imaging and time reversal

- Imaging and time reversal in random media in which there is **significant multipathing**.
  - Foliage penetrating and ground penetrating radar.
  - Identification of underground or underwater mines and structures.
  - Non destructive testing for locating defects in concrete, airplane structures, etc.
  - Secure communication in cluttered environments.

.

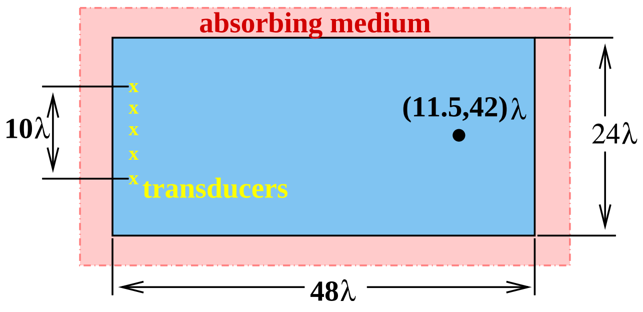

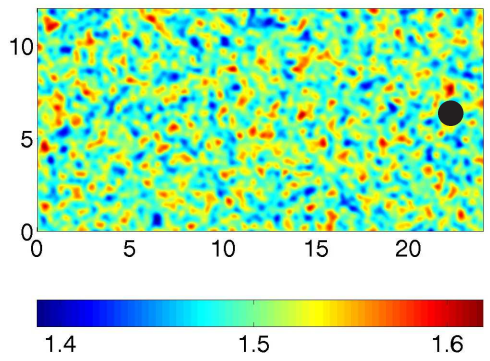

- Targets are simulated as soft scatterers (Dirichelt BC at their surface).
- **Ultrasound probing:** $\lambda = 0.5$mm, $a = 2.5$mm (5mm), $c_0 = 1.5$km/s.
- **Underwater sound:** scale lengths by $\sim 10^3$. $\lambda \sim 1$m, $L = 1 - 50$km, $a = 50 - 100$m.
- **Radar** microwaves: scale lengths by $\sim 10^2$. $\lambda = 10 - 30$cm, $L \sim 1$km, $a = 1 - 10$ m.

• A target $\mathbf{y}_1$ illuminates the array. The recorded signal is time reversed (conjugated in Fourier domain) and sent into medium.

The back propagated field at observation point $\mathbf{y}$ is

$$\Gamma(\mathbf{y},\mathbf{y}_1,t) = \int e^{-i\omega t} \sum_{j=1}^{N} \widehat{G}(\mathbf{y},\mathbf{x}_j,\omega)\overline{\widehat{f}}(\omega)\overline{\widehat{G}}(\mathbf{y}_1,\mathbf{x}_j,\omega)d\omega$$

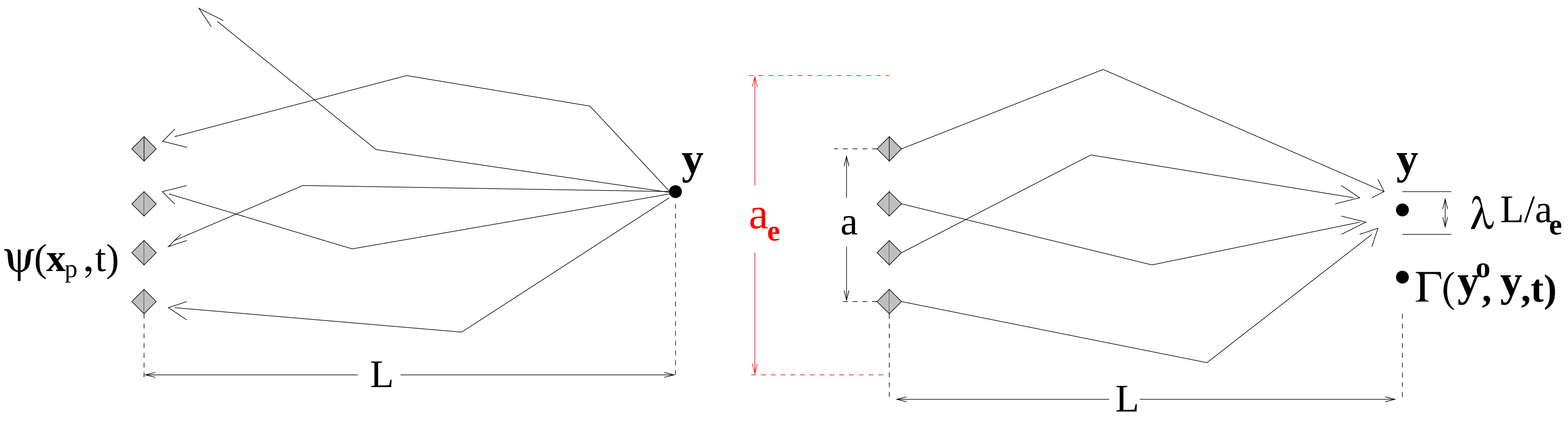

• **Super-resolution** In a random medium the refocusing is much tighter. Multipathing gives effective aperture $a_e \gg a$ or, $\frac{\lambda L}{a_e} \ll \frac{\lambda L}{a}$.

Self averaging of back propagated field $\Gamma(\mathbf{y}, \mathbf{y}_1, t)$

- Decorrelation of $\widehat{\Gamma}(\mathbf{y}, \mathbf{y}_1, \omega) = \overline{\widehat{f}}(\omega) \widehat{G}(\mathbf{y}, \mathbf{x}_j, \omega) \overline{\widehat{G}}(\mathbf{y}_1, \mathbf{x}_j, \omega)$ for frequencies $\omega_1 \neq \omega_2$ gives

$$E\left\{\Gamma^2(\mathbf{y}, \mathbf{y}_1, t)\right\} \approx E\left\{\Gamma(\mathbf{y}, \mathbf{y}_1, t)\right\}^2 .$$

- Back propagated field is **self averaging**: $\Gamma(\mathbf{y}, \mathbf{y}_1, t) \approx E\left\{\Gamma(\mathbf{y}, \mathbf{y}_1, t)\right\}$.

- The analytic expression for $\Gamma(\mathbf{y}, \mathbf{y}_1, t)$ coincides with the expression for the back propagated field in a homogeneous medium, for an array of **effective aperture** $\mathrm{a_e} \gg \mathrm{a}$.

- Self-averaging and super-resolution are observed **in time** and not for monochromatic fields. Broadband is essential.

Simulation of super-resolution.

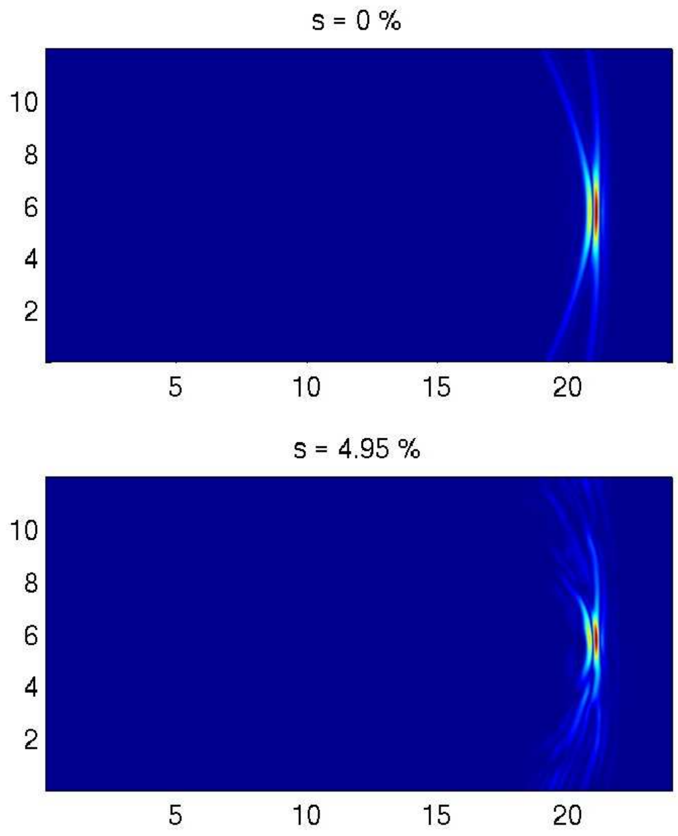

$s =$ standard deviation of the fluctuations of sound speed.

Imaging in random media

- We use the statistical stability and the super-resolution of time reversal in random media, for imaging.

- To identify the unknown targets, we construct objective functions which are self-averaging.

- There are two stages in our imaging approach:

  1. Statistically stable direction of arrival estimation.

  2. Coherent imaging. Using the phase or arrival time info.

- We show numerical simulations & comparison with other, frequently used methods (narrow-band beamforming (MUSIC) and SAR).

Imaging. Forward model of response matrix P, at frequency ω.

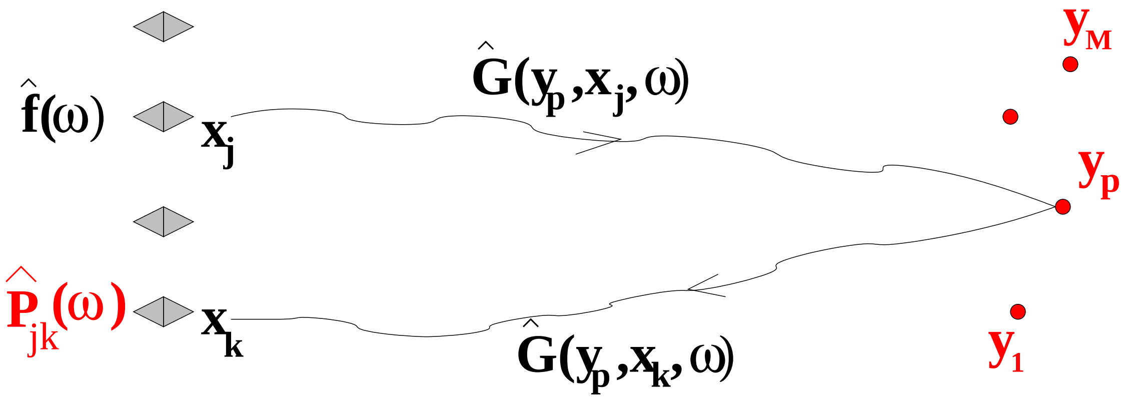

$\widehat{P}_{jk}(\omega) =$ sum of fields scattered from all targets $\mathbf{y}_p$, $p = 1, \ldots M$.

We neglect multiple scattering.

- $\widehat{P}(\omega) = \widehat{f}(\omega) \sum_{p=1}^{M} \widehat{\tau}_p(\omega) \widehat{\mathbf{g}}(\mathbf{y}_p, \omega) \widehat{\mathbf{g}}^T(\mathbf{y}_p, \omega)$, $\widehat{\mathbf{g}}(\mathbf{y}_p, \omega) = \begin{pmatrix} \widehat{G}(\mathbf{y}_p, \mathbf{x}_1; \omega) \\ \vdots \\ \widehat{G}(\mathbf{y}_p, \mathbf{x}_N; \omega) \end{pmatrix}$

$\widehat{\tau}_p(\omega)$ =scattering coefficient of target p.

- rank $\left[\widehat{P}(\omega)\right] = M \leq N$, except for very special configurations of targets and transducers.

SVD of $\widehat{P}(\omega)$. Statistically stable imaging.

- M = number of significant singular values $\sigma_j(\omega)$.
- The left singular vectors $\widehat{\mathbf{V}}_j$, for $j = 1, \dots M$, are linear combinations of $\widehat{\mathbf{g}}(\mathbf{y}_p, \omega)$, the random, illuminating Green's vectors.

Imaging M targets

For search point $\mathbf{y}$, if projection onto the null space of $\widehat{P}(\omega)$, $\mathcal{P}_N \widehat{\mathbf{g}}(\mathbf{y}, \omega) = 0$, then $\mathbf{y} = \mathbf{y}_p$, for some $p = 1, \dots M$.

In imaging, $\widehat{\mathbf{g}}(\mathbf{y}, \omega)$ is unknown. Use the deterministic $\widehat{\mathbf{g}}_0(\mathbf{y}, \omega)$ instead.

$$\mathbf{F}(\mathbf{y}, t) = \int e^{-i\omega t} \mathcal{P}_N \widehat{\mathbf{g}}_0(\mathbf{y}, \omega) d\omega.$$

• Minima of $| \, \mathbf{F}(\mathbf{y}, t) \, | \Longrightarrow$ information about location of targets. It works because $\mathbf{F}(\mathbf{y}, t)$ is self-averaging.

Connection between imaging and time reversal

For simplicity of explanation, take one target. It extends to multiple targets, with modifications.

- For a search point $\mathbf{y}$, we calculate

$$\mathbf{F}(\mathbf{y},t) = \int e^{-i\omega t} \left\{ \left[\widehat{\mathbf{V}}_1^H(\omega) \hat{\mathbf{g}}_0(\mathbf{y},\omega) \right] \widehat{\mathbf{V}}_1(\omega) - \mid \widehat{\mathbf{V}}_1(\omega) \mid^2 \hat{\mathbf{g}}_0(\mathbf{y},\omega) \right\},$$

where we normalized $\widehat{\mathbf{V}}_1(\omega)$ with the singular value $\sigma_1(\omega)$ such that $\widehat{\mathbf{V}}_1(\omega) \sim \mid \widehat{f}(\omega) \mid^{\frac{1}{2}} \hat{\mathbf{g}}(\mathbf{y}_1,\omega)$.

Each term in $\mathbf{F}(\mathbf{y},t)$ has a time reversal interpretation and is self-averaging.

$$\mathbf{F}^{(1)}(\mathbf{y},t) = \int e^{-i\omega t} \mid \widehat{V}_1(\omega) \mid^2 \widehat{\mathbf{g}}_0(\mathbf{y},\omega) d\omega =$$

$$\int e^{-i\omega t} \mid \widehat{f}(\omega) \mid \widehat{\mathbf{g}}_0(\mathbf{y},\omega) \sum_{j=1}^{N} \overline{\widehat{G}}(\mathbf{y}_1,\mathbf{x}_j,\omega) \widehat{G}(\mathbf{y}_1,\mathbf{x}_j,\omega) d\omega.$$

Echos received from unknown target y_1 in random medium

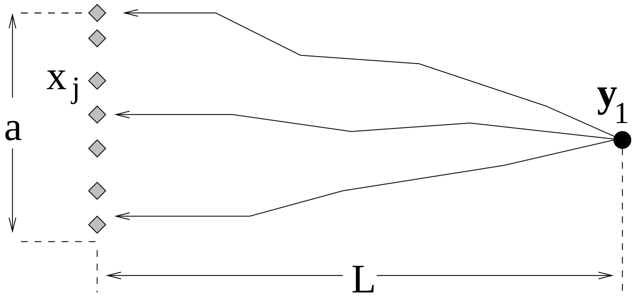

TR and resend into random medium

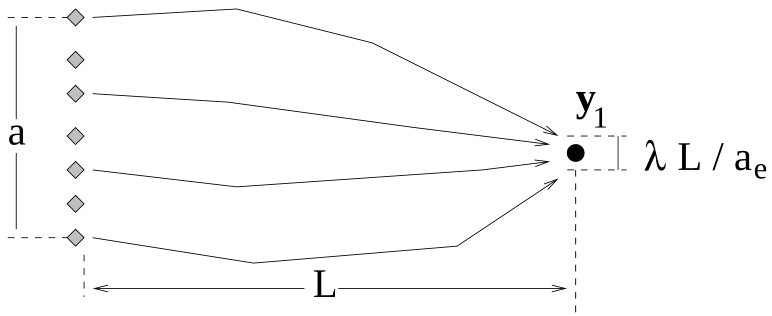

Search point y illuminates the array in fictitious homogeneous medium

Eval. $F^{(1)}$ at deterministic time. (self−averaging).

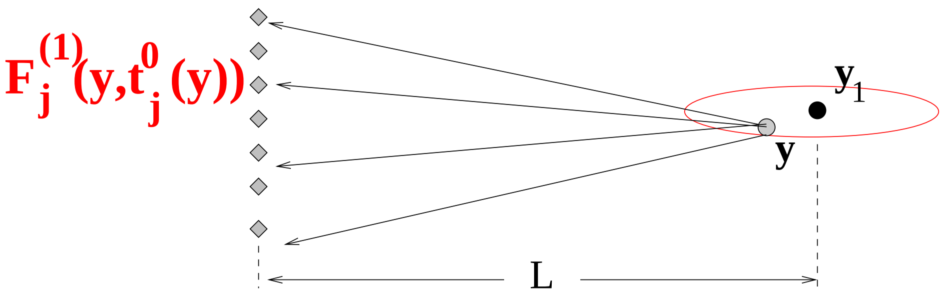

$$\mathbf{F}^{(2)}(\mathbf{y},t) = \int e^{-i\omega t}\left[\widehat{\mathbf{V}}_1^H(\omega)\widehat{\mathbf{g}}_0(\mathbf{y},\omega)\right]\widehat{\mathbf{V}}_1(\omega)d\omega =$$

$$\int e^{-i\omega t} \mid \widehat{f}(\omega) \mid \widehat{\mathbf{g}}(\mathbf{y}_1,\omega)\sum_{j=1}^{N}\overline{\widehat{G}}(\mathbf{y}_1,\mathbf{x}_j,\omega)\widehat{\mathbf{G}}_0(\mathbf{y},\mathbf{x}_j,\omega)d\omega.$$

Echos received from unknown target y_1 in random medium.

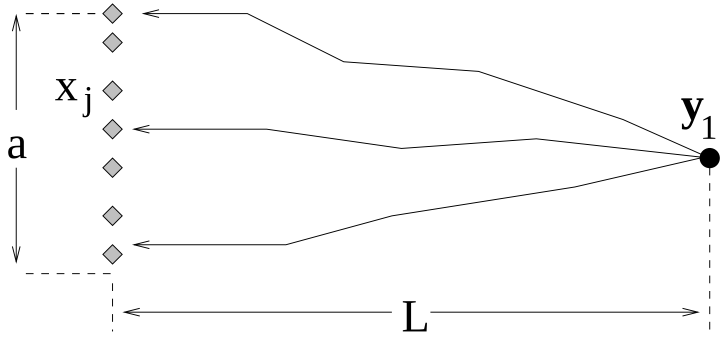

TR and propagate to search point y in fictitious homog. med.

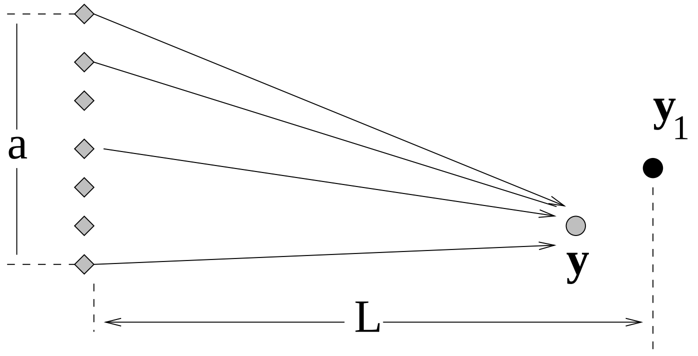

Illuminate the array from unknown y_1 in the random medium

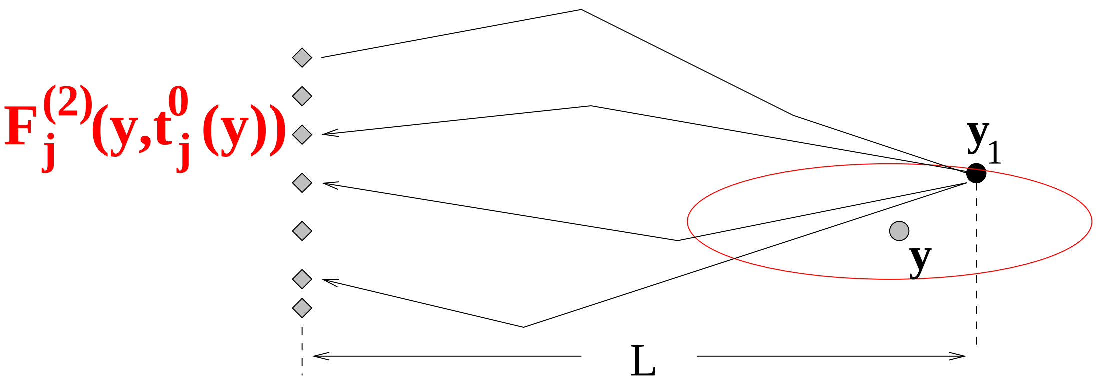

Direction of arrival estimation I.

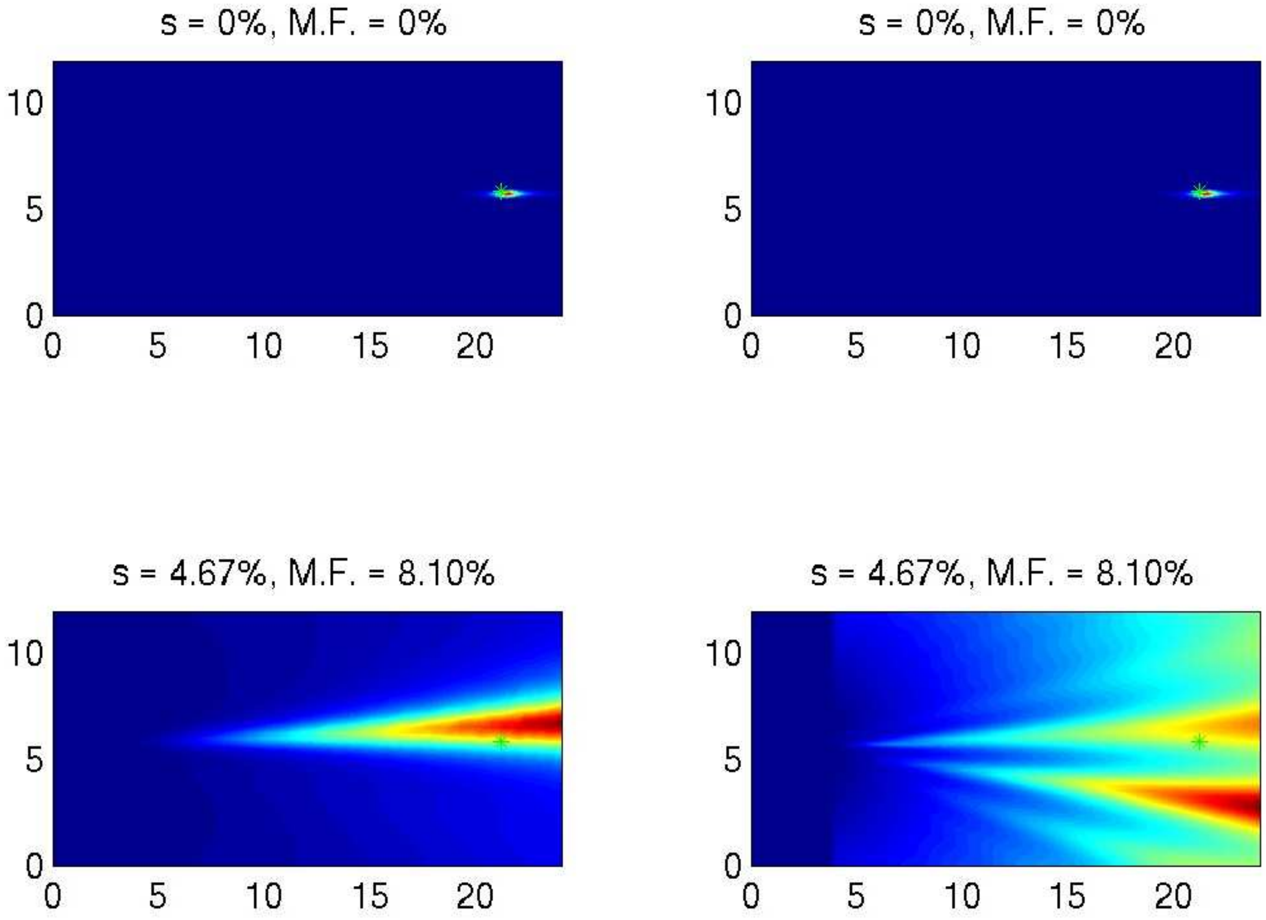

On the left time domain estimation, on the right fixed frequency MUSIC.

Direction of arrival estimation II

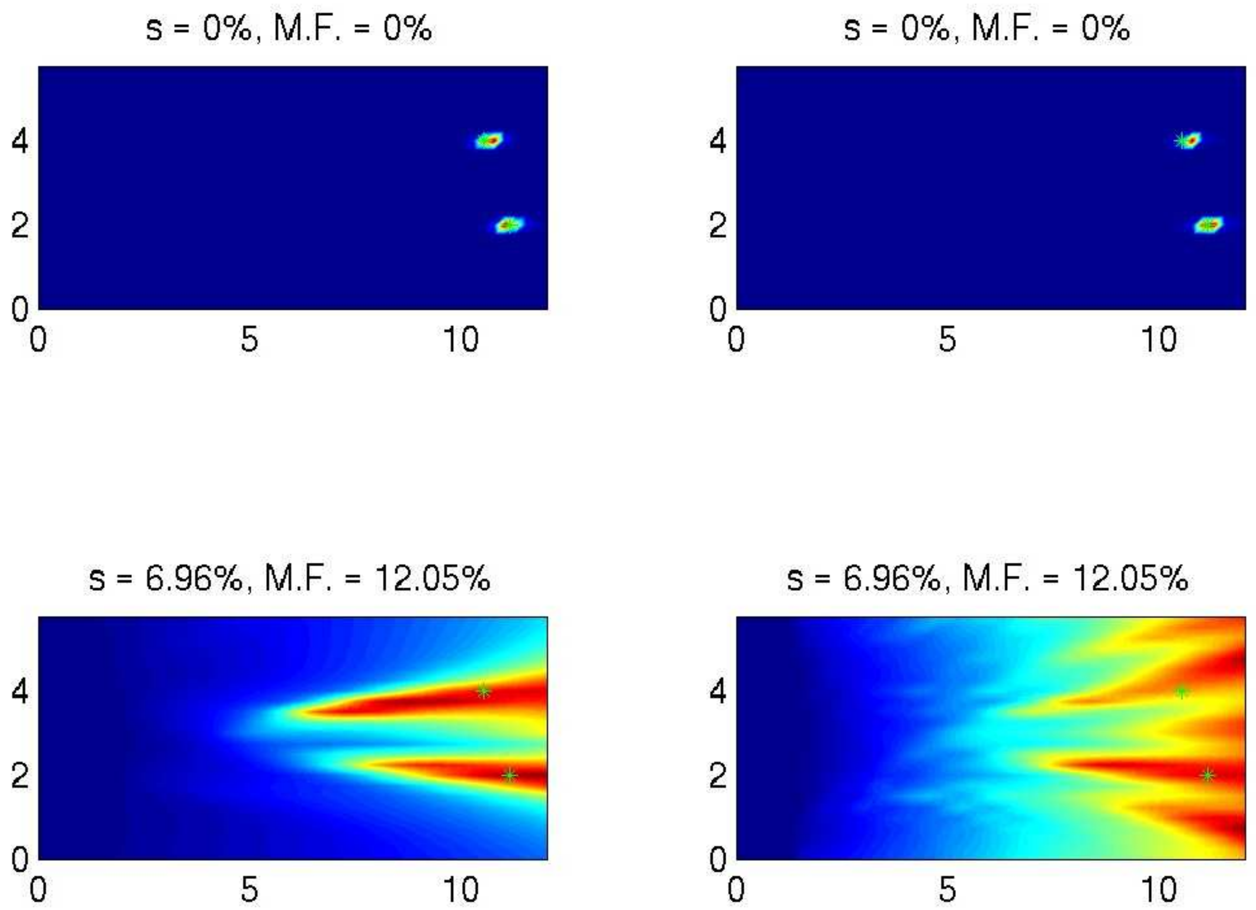

On the left time domain estimation, on the right fixed frequency MUSIC.

Sensitivity of time domain direction of arrival estimation to arrival times used.

- Get very bad range estimation when using deterministic arrival times
- Using estimated arrival times improves cross range estimation greatly
- Need for good arrival time estimation

Coherent imaging: target range estimation

The phase (arrival time) in the data gives the range of targets.

Traditional arrival time analysis. SAR

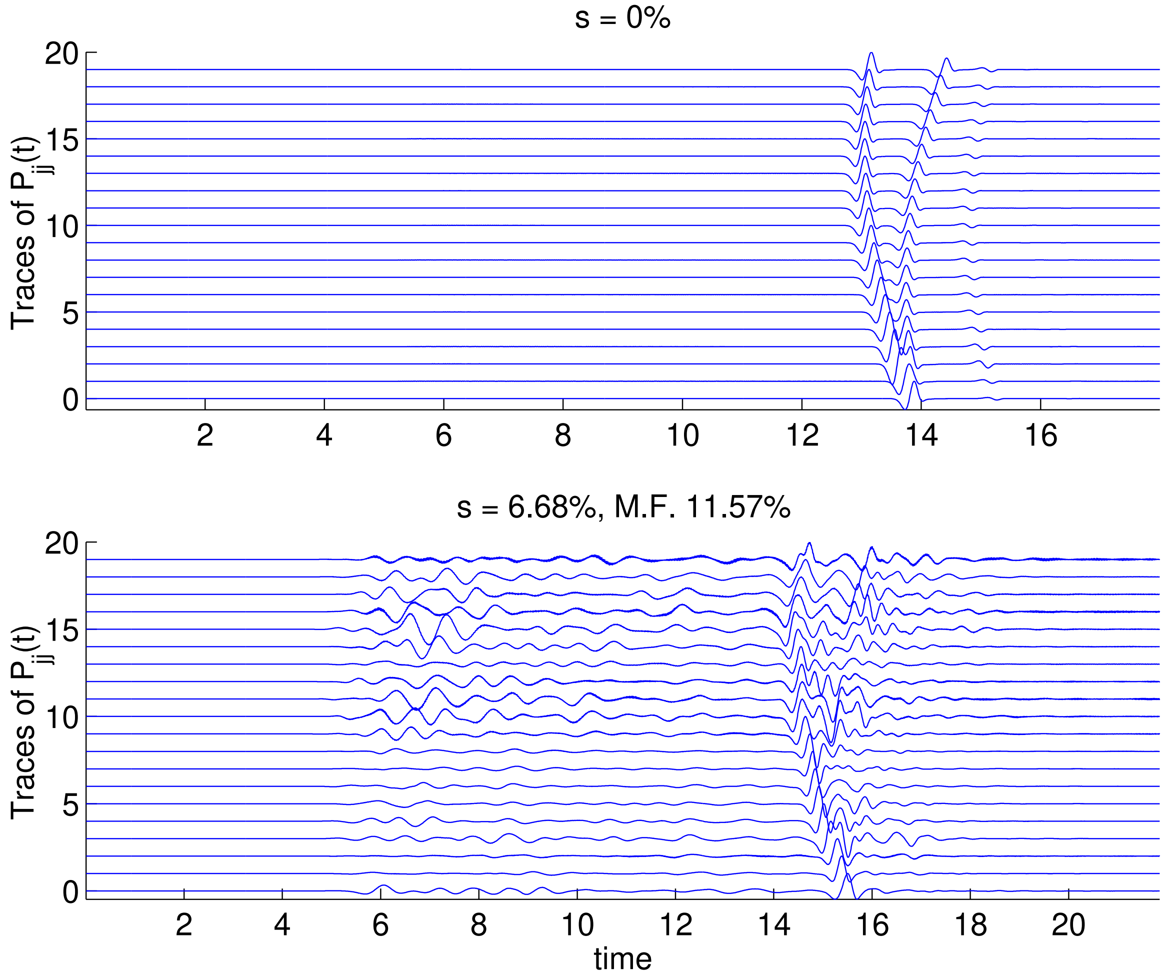

ATA imaging of two targets in a random medium.

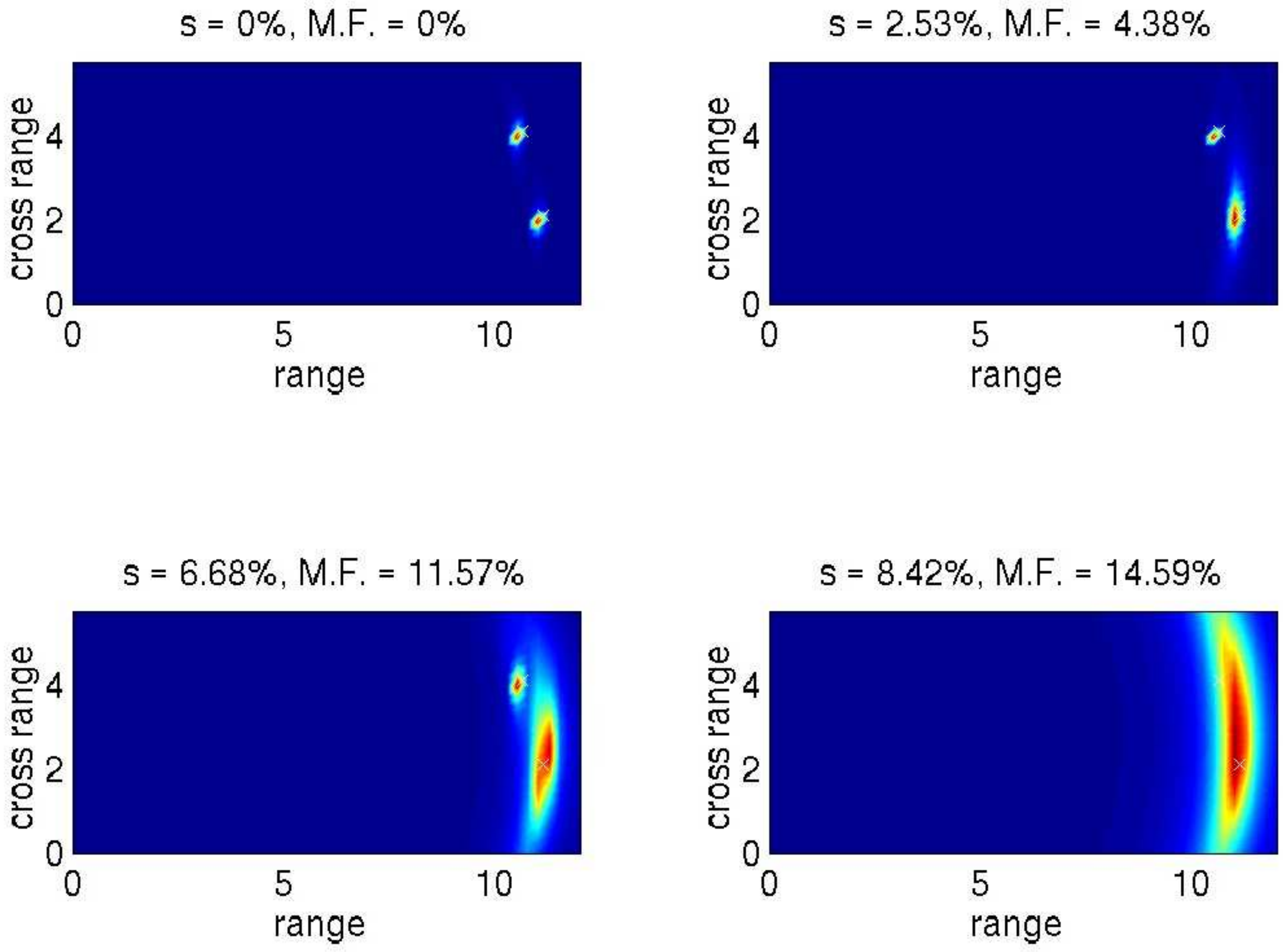

Using **only** arrival time information and LSQ fitting of hyperbolas (common in seismic imaging).

Subspace - Arrival Time (SAT) analysis

- Singular vectors are also used to get better range estimates. (Illuminate one target and shade the other).

- SVD gives complex, singular vectors $\widehat{\mathbf{V}}_j(\omega)$ up to arbitrary, $e^{i\phi(\omega)} \Longrightarrow \int e^{-i\omega t}\widehat{\mathbf{V}}_j(\omega)d\omega$ is not coherent in time.

- Calculate N coherent in time vectors:

$$\mathbf{v}_j^{(m)}(t) = \int e^{-i\omega t}\left[\widehat{\mathbf{V}}_j^H(\omega)\cdot\widehat{P}(\omega)\mathbf{e}_m\right]\widehat{\mathbf{V}}_j(\omega)d\omega.$$

Equivalent to taking m^{th} column of $P(t)$, time reverse it and send it into the medium. Repeat this an infinite number of times.

- Stack the $\mathbf{v}_j^{(m)}(t)$ to get better estimates of arrival times.

$$\left\langle \mathbf{v}_j(t)\right\rangle = \frac{1}{N}\sum_{j=1}^{N}\mathbf{v}_j^{(m)}(t-\tau_m), \qquad \min_{\tau_m}\int_0^T\sum_{m=1}^{N}\left[\mathbf{v}_j^{(m)}(t-\tau_m)-\left\langle\mathbf{v}_j(t)\right\rangle\right]^2.$$

Traces for random medium with st. dev. $s = 6.68\%$

(a1) 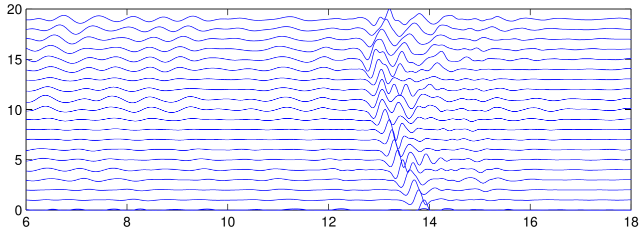

(b1) 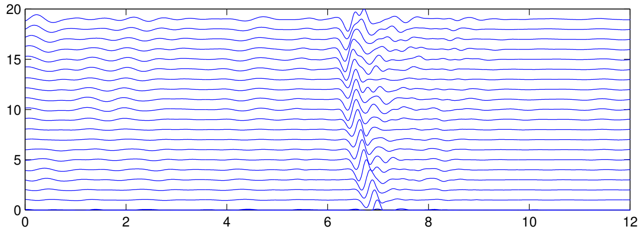

(a2) 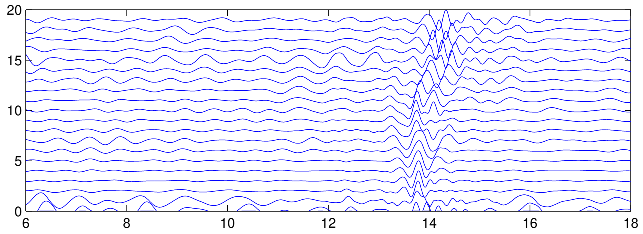

(b2) 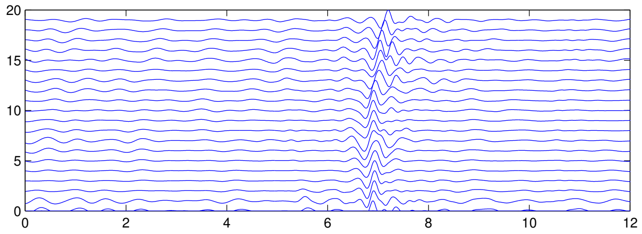

(c) 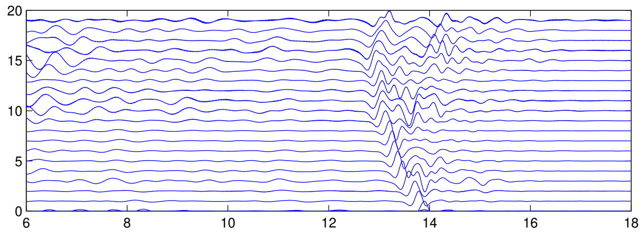

(a1) traces of m^{th} component of $\mathbf{v}_1^{(m)}(t)$, $m = 1, \ldots N$.

(a2) traces of m^{th} component of $\mathbf{v}_2^{(m)}(t)$, $m = 1, \ldots N$.

(b1) and (b2): traces of $\langle \mathbf{v}_1(t) \rangle$ and $\langle \mathbf{v}_2(t) \rangle$.

(c) traces of $P_{jj}(t)$.

The SAT estimation

- The SAT objective function is basically an intersection between SVD direction of arrival estimation and subspace arrival time analysis.

- The D-o-A estimation gives good cross-range resolution of the targets.

- The subspace arrival time analysis gives good range resolution of each target.

- The intersection gives good cross-range and range resolution.

SAT imaging of one target in a random medium

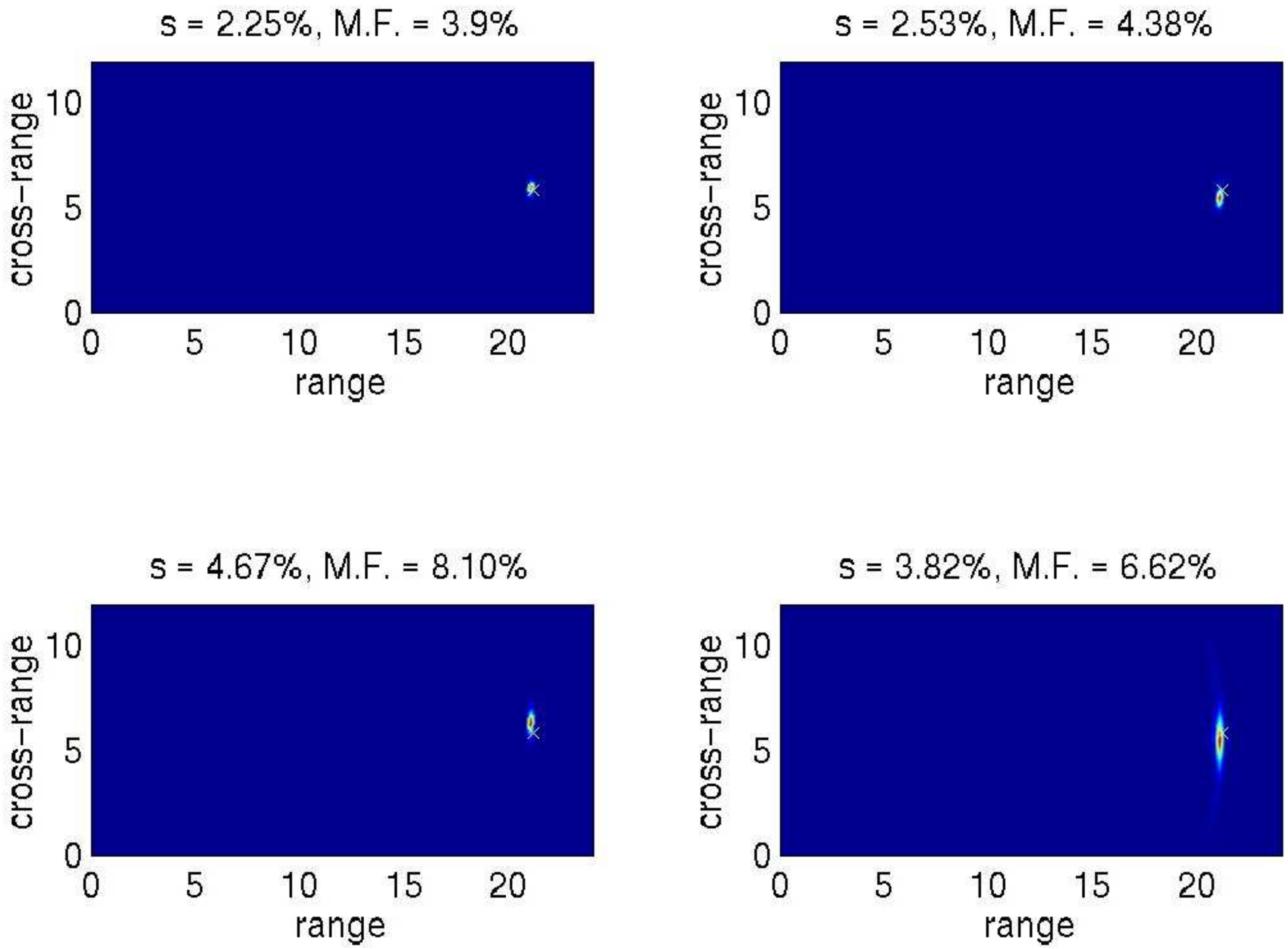

s = standard deviation, M.F. = max. fluctuations of sound speed

SAT imaging of two targets in a random medium

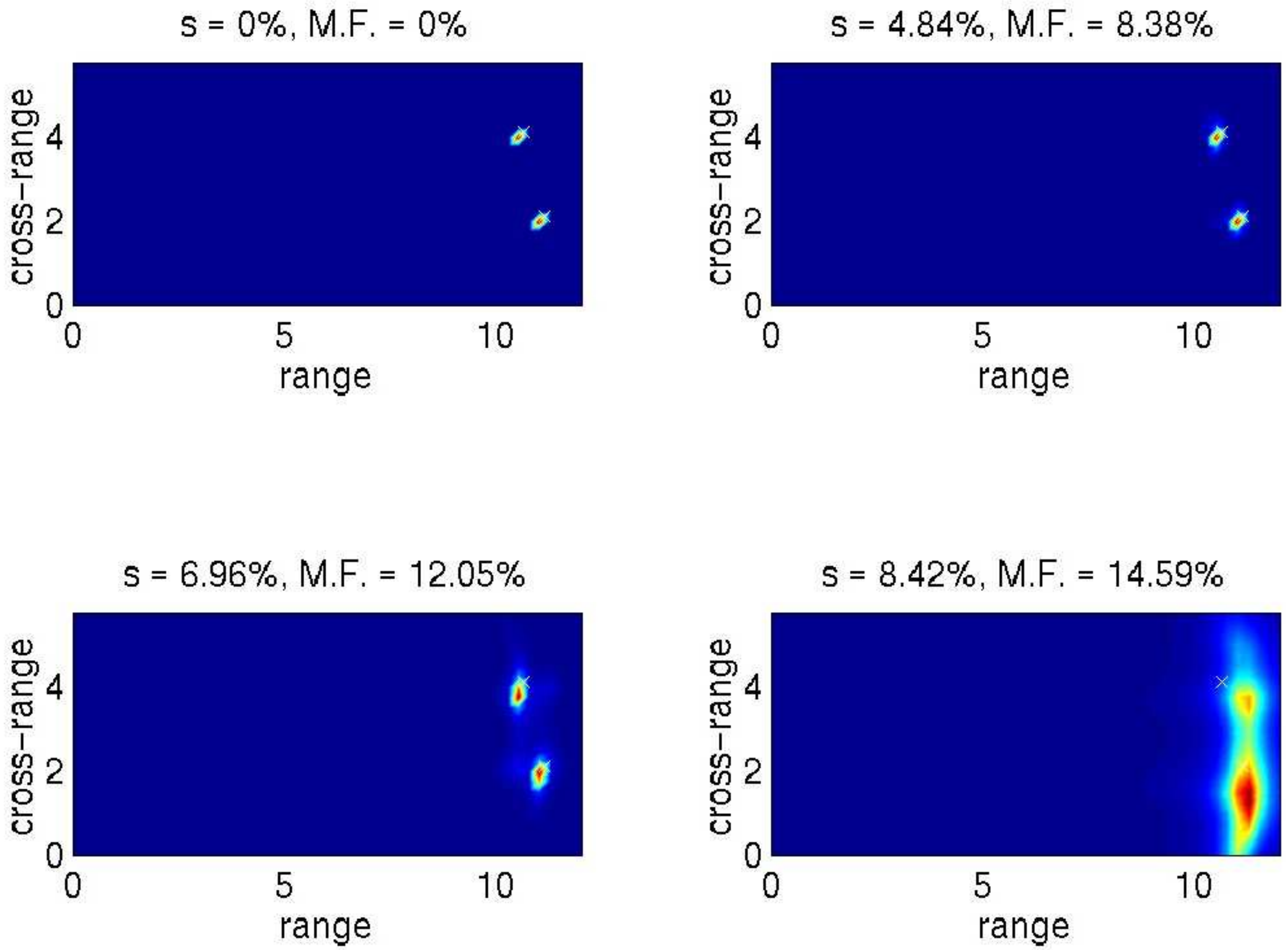

s = standard deviation, M.F. = max. fluctuations of sound speed

Why SAR gives does not work in a random medium

- SAR is when only the **diagonal** $P_{jj}(t)$ of the response matrix is measured.

- Maxima of

$$\mathcal{R}(\mathbf{y}^s) = \sum_{j=1}^{N} P_{jj}\left(\frac{2|\mathbf{x}_j - \mathbf{y}^s|}{c_0}\right)$$

  give target estimates.

- No projection, no ‘time reversal’, no statistical stability.

One target SAR in a random medium

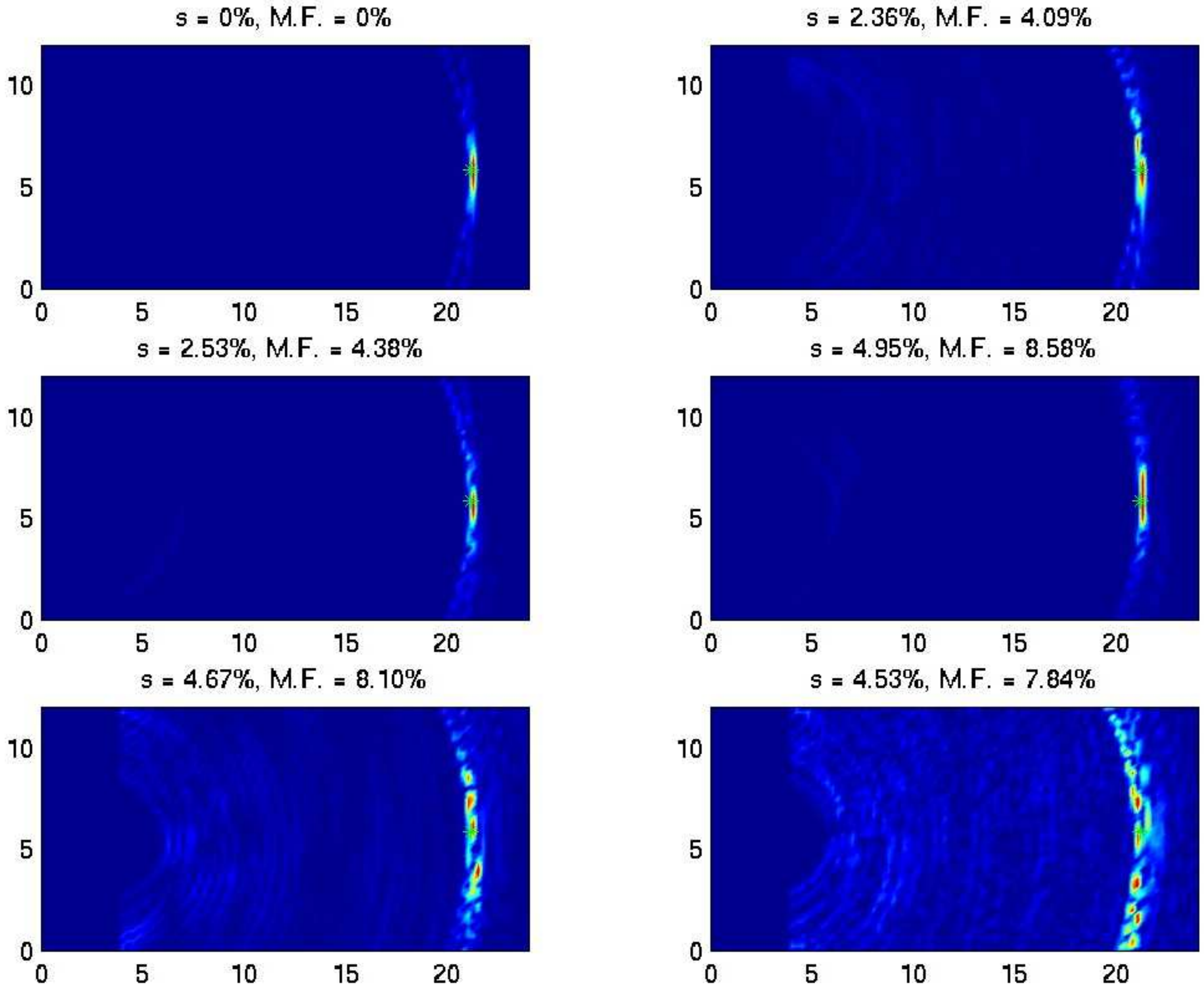

- Our success in imaging in random media is due to the **self-averaging** property of the objective functionals.

- The random part of the functionals is of the form

$$\Gamma(z;\mathbf{x},\mathbf{y};\xi,\eta,t) = \int e^{-i\omega t}\widehat{f}(\omega)\widehat{G}(z,0;\mathbf{x},\xi;\omega)\overline{\widehat{G}}(z,0;\mathbf{y},\eta;\omega)d\omega$$

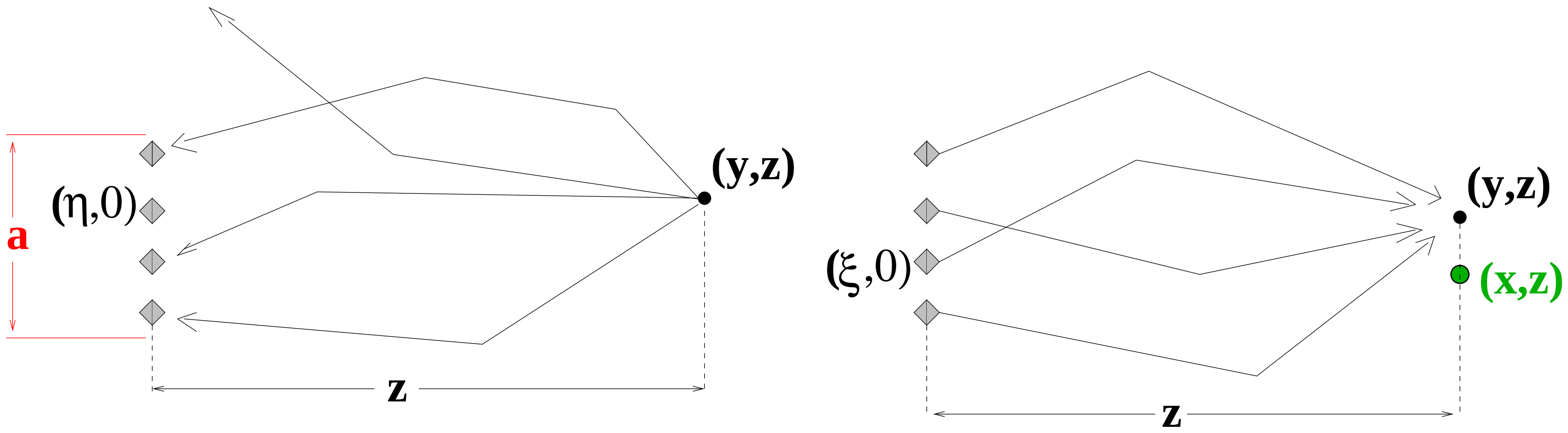

$|\,\mathbf{x}\,|$, $|\,\mathbf{y}\,|$ are $O(a)$, $|\,\mathbf{x}-\mathbf{y}\,|$ is small and $z \sim L$, the propagation distance.

Analysis of statistical stability

• For long propagation distances L and weak sound velocity fluctuations (forward scattering), use the parabolic Green's function:

$$\begin{cases} 2ik\frac{\partial \widehat{G}}{\partial z} + \Delta_{\mathbf{x}}\widehat{G} + k^2\sigma\mu\left(\frac{\mathbf{x}}{l}, \frac{z}{l}\right)\widehat{G} = 0, \text{ for } z > 0, \\ \widehat{G} = \delta(\mathbf{x} - \xi) \text{ at } z = 0. \end{cases}$$

σ is the standard deviation of the fluctuations $\mu(\mathbf{x}, z) = \frac{c_0^2}{c(\mathbf{x},z)^2} - 1$.

• In a regime $L \gg a \gg l$ and weak fluctuations (σ small) $\to$ the white noise limit (convergence in law):

$$d\widehat{G} = \left[\frac{i}{2k}\Delta_{\mathbf{x}}\widehat{G} - \frac{k^2}{8}R_0(0)\widehat{G}\right]dz + \frac{ik}{2}\widehat{G}\; dB(\frac{\mathbf{x}}{l}, z), \text{ for } z > 0.$$

• $B(\mathbf{x}, z)$ is a field of Brownian motions in z, with covariance

$$E\left\{B(\mathbf{x}_1, z_1)B(\mathbf{x}_2, z_2)\right\} = R_0(\mathbf{x}_1 - \mathbf{x}_2)z_1 \bigwedge z_2,$$

$$R_0(r) = \int R(r, z)dz, \; R(r, z) = E\left\{\mu(r + r', z + z')\mu(r, z)\right\}.$$

$$\begin{cases} d\widehat{\Gamma} = \left\{ \frac{i}{2k} \left(\Delta_{\mathbf{x}} - \Delta_{\mathbf{y}}\right) \widehat{\Gamma} + \frac{k^2}{4} \left[R_0(\frac{\mathbf{x}}{l} - \frac{\mathbf{y}}{l}) - R_0(0) \right] \widehat{\Gamma} \right\} dz + \\ \qquad \frac{ik}{2} \widehat{\Gamma} \left[dB(\frac{\mathbf{x}}{l}, z) - dB(\frac{\mathbf{y}}{l}, z) \right], \text{ for } z > 0, \\ \widehat{\Gamma} = \delta(\mathbf{x} - \xi)\delta(\mathbf{y} - \eta), \quad \text{at } z = 0. \end{cases}$$

- We are interested in points $\mathbf{x}$ and $\mathbf{y}$ that are close together, such that $\mathbf{Y} = \mathbf{y} - \mathbf{x}$ satisfies $|\,\mathbf{Y}\,| \ll l$.

- Also, if $\mathbf{X} = \frac{1}{2}(\mathbf{x} + \mathbf{y})$ is the center point, then $|\,\mathbf{X}\,| \gg l$. In particular, $\frac{l}{a} = \epsilon \ll 1$.

- Take the Fourier transform with respect to Y and define the Wigner distribution:

$$W = \int e^{i\mathbf{P}\cdot\mathbf{Y}} \widehat{\Gamma}(z; \mathbf{X}, \mathbf{Y}; \xi, \eta, k) d\mathbf{Y},$$

Statistical stability

- After a rescaling, we obtain the Ito Liouville equation

$$\begin{cases} dW = \{-\mathbf{P}\cdot\nabla_{\mathbf{X}}W + D\Delta_{\mathbf{P}}W\}\,dz - \frac{1}{2}\nabla_{\mathbf{P}}W\cdot d\nabla_{\mathbf{X}}B(\frac{\mathbf{X}}{k^3\epsilon}, z), \\ \\ W = e^{i\mathbf{P}\cdot(\eta-\xi)}\,\delta\left(\mathbf{X}-\frac{\xi+\eta}{2}\right) \quad \text{at } z=0; \quad D = -\Delta R_0(\mathbf{X})\,|_{\mathbf{X}=\mathbf{0}}\,. \end{cases}$$

- Decorrelation of W or $\widehat{\Gamma}$, at different frequencies.

The coupling term in the equation for $W(X,P,z;k_1)W(X,P,z;k_2)$ is in terms of

$$R_0\left(\frac{\mathbf{X}}{k_1^3\epsilon}-\frac{\mathbf{X}}{k_2^3\epsilon}\right)\approx 0, \quad \text{since } \epsilon \ll 1.$$

- Self-averaging in time of $\Gamma = \int d\omega \int d\mathbf{P} e^{-i(\omega t+\mathbf{P}\cdot\mathbf{Y})}W$ follows.

Conclusions and future research

• We have introduced and explored with simulations a theory for super-resolution and statistical stability of time reversal in random media.

• We have introduced a coherent array imaging method for target identification in random media, which exploits the super-resolution and statistical stability of time reversal.

Research plans

- Apply to foliage and ground penetrating radar
- Imaging with very large, moving (synthetic) arrays. Hierarchical, multiscale methods for analyzing very large response matrices.
- Multipathing in wireless for secure communications in a cluttered environment.